



Reliability of Moment Tensor Inversion for Different Seismic Networks

ANNA TYMIŃSKA¹ and GRZEGORZ LIZUREK¹

Abstract—The article investigates the reliability of moment tensor (MT) inversion in time domain with use of first P-wave amplitude, a method used to determine the source mechanisms of earthquakes, across four different seismic networks. The study compares the synthetic tests results of MT inversion for two underground mining and two artificial reservoir monitoring seismic networks. The analysis was performed to assesses how consistency and accuracy of the results depend on different factors like: network configuration, events depth, velocity model, focal mechanism of event and applied noise. The findings highlight the impact of network configuration compared to other variables and data quality on the reliability of moment tensor inversion and provide insights into different factors which have to be considered to enhance MT accuracy. The significance of events depth in P-wave amplitude MT inversion and the necessity to consider velocity model influence, especially presence of high velocity gradient, is highlighted by the presented results.

Keywords: Focal mechanism, anthropogenic seismicity, moment tensor inversion, synthetic tests, noise influence.

1. Introduction

Seismic moment tensor (MT) is an important value in earthquake foci analysis. MT gives an information about mechanism in terms of type of crack and forces prevalence on fault. Such features of the MT allow the analysis of focal mechanism in both tectonic and anthropogenic seismic events. MT provides information for creating tectonic models and seismogenic settings in observed area (D'Amico, 2018). Inversion of MT is routinely applied for analysis of strong natural earthquakes (Ekstrom et al., 2012), but also for regional, local natural events and induced earthquakes (np. Cesca et al., 2006). In

anthropogenic seismicity, MT inversion is used as the tool for estimation if the event was triggered or induced (i.e. Fletcher & McGarr, 2005; Ford et al., 2009). Interpretation of MT solutions allows for determination of main stress axes in tectonic active regions (Hardebeck & Michael, 2006) and anthropogenic seismicity areas (Martinez-Garzon et al., 2014). MT decomposition because of distinguishing isotropic part (ISO), compensated linear vector dipole component (CLVD) and pure shear (DC) is used in analysis of focal mechanism of such events as volcanic tremors, meteor impacts or nuclear explosion (np. Cesca et al., 2013; Heimann et al., 2013; Vavryčuk & Kim, 2014). Based on MT solutions for different earthquakes in mining seismicity the non-DC components of full mechanisms became an indicator of the induced character of tremor (Dahm et al., 2013). As was showed MT provide vital information for studying the physics of seismic source. Therefore, limitations of this method require careful interpretation of the results after matching the most proper method of the inversion.

Seismic moment tensor (MT) inversion methods are based on the full waveform inversion or amplitude inversion (Zahradnik & Sokos, 2018; Kwiatek et al., 2016). All methods require good quality data. As Bentz et al. (2018) showed the inversion for small earthquakes are more robust for the amplitude inversion. Also the more accurate results are obtained for first P-wave amplitude inversion if the non-shearing components occur (Fojtikowa et al., 2010). The presence of the non-shearing components is considered as an effect of the wave anisotropy radiation in case of strong natural earthquakes (Vavryčuk, 2018) or the influence of other factors: seismic noise (e.g. Šílený et al., 2014), velocity model uncertainties (e.g. Romanowicz et al., 1993) and stations focal coverage (e.g. Ford et al., 2010).

¹ Institute of Geophysics Polish Academy of Sciences, Księcia Janusza 64, 01-452 Warsaw, Poland. E-mail: atyminska@igf.edu.pl

Therefore, non-DC components are used as the determinant for the anthropogenic earthquakes, where isotropic or uniaxial forces are more probable to occur (Gibowicz & Kijko, 1994; Rudajev & Šílený, 1985; Miller et al., 1998). We decided to use the first P-wave amplitude inversion in time domain (Wiejacz, 1992; Kwiatek et al., 2016) for the influence of noise contamination and station focal coverage analysis. The main aim to perform synthetic tests was the assessment of reliability of seismic moment tensor inversion for non-DC sources. Synthetic tests were performed to check the influence of noise contamination with depth of seismic source for normal and thrust faults for four surface networks: two for underground mines monitoring and two for artificial reservoir monitoring.

2. Site Characteristics

ViEtnam Reservoir Induced Seismicity (VERIS) network was established to monitor seismic activity triggered by artificial reservoir. The Song Tranh 2 reservoir is placed in central Vietnam on Tranh river. Before the reservoir impoundment region was recognized as aseismic with few small earthquakes noticed from the XVII century, strongest noticed event has magnitude $M = 4.7$. Reservoir impoundment started in November 2010 and since the beginning of 2011 seismic activity rate increased (Wisznowski et al., 2015). Seismic network was developed and was compound of up to 10 stations during the highest activity period. Seismicity in the vicinity of Song Tranh 2 reservoir is characterised by the seasonal trends dependent on the wet and dry season and the water level of the reservoir (Lizurek et al., 2021). The largest earthquakes in the area were September 3, 2012 M4.2, October 22, 2012 M4.6 and November 15, 2012 M4.7. Events are located in close vicinity and beneath the reservoir and less often on existing faults (Fig. 1). The velocity model in this area is isotropic, as it reflects the crystalline base (Fig. 3). Obtained focal mechanisms were usually normal faults with prevalence of the shearing component (see Fig. 1 and Fig. 9 in Lizurek et al., 2017). More details about the seismic activity of the area are described recently by Gahalaut et al. (2016) and

Lizurek et al. (2017). All data, including moment tensor (MT) solutions, are available in the EPI-SODES platform (IS-EPOS, 2017a, 2017b).

Lai Chau seismic network was set up for artificial reservoir monitoring in Lai Chau province, northern Vietnam. Network was established in 2014 before impoundment of the reservoir and developed in next years, currently consists of up to 10 seismic stations located 4–112 km from each other. Location of seismic stations depended strongly on existing roads and urbanisation, what causes poor coverage of the area to the west from the reservoir. Background seismicity is connected mostly with Nam Nho-Nam Cuoi and Moug Te fault zones, but also events near the dam were registered in 8 months period before impoundment. Filling up the reservoir started in June 2015 and finished in July 2016. There was decrease of the seismic activity directly after impoundment. The maximum registered magnitude was $M_L 5.1$ in August, 13, 2018 (Lizurek et al., 2019). Events occurred at depth 4–15 km. The velocity model changes gradually with depth (Fig. 3). Data from Lai Chau network allowed for calculating 12 MT solutions with the use of first P-wave amplitude inversion. Obtained mechanisms were mostly shearing normal and strike-slip faults. All data, including moment tensor (MT) solutions, are available in the EPI-SODES platform (IS-EPOS, 2018).

LUMINEOS network is surface seismic network settled to monitor seismicity in Rudna copper mine. Rudna mine is located in south-west Poland in Legnica-Głogów Cooper District (LGOM). In Rudna ore is exploited in chamber-pillar system at depth 600–900 m. Geologic structure is simple with overlying strata and layers slightly dipping to northeast. Below the excavation level there is low velocity anhydrite layer (Fig. 3). Seismicity in this region is induced by mining and its connected with the rate and area of exploitation (Lasocki & Orlecka-Sikora, 2008). Every year in this area more than 1000 events with magnitude $M > 1$ are recorded which makes LGOM the most seismic area in Poland. Mechanisms of tremors are also connected with mining works and mostly non-shearing character of events is visible (Fig. 2). Seismic data are available on Episodes Platform (IS-EPOS, 2017a, 2017b).

Reliability of Moment Tensor Inversion for Different Seismic Networks

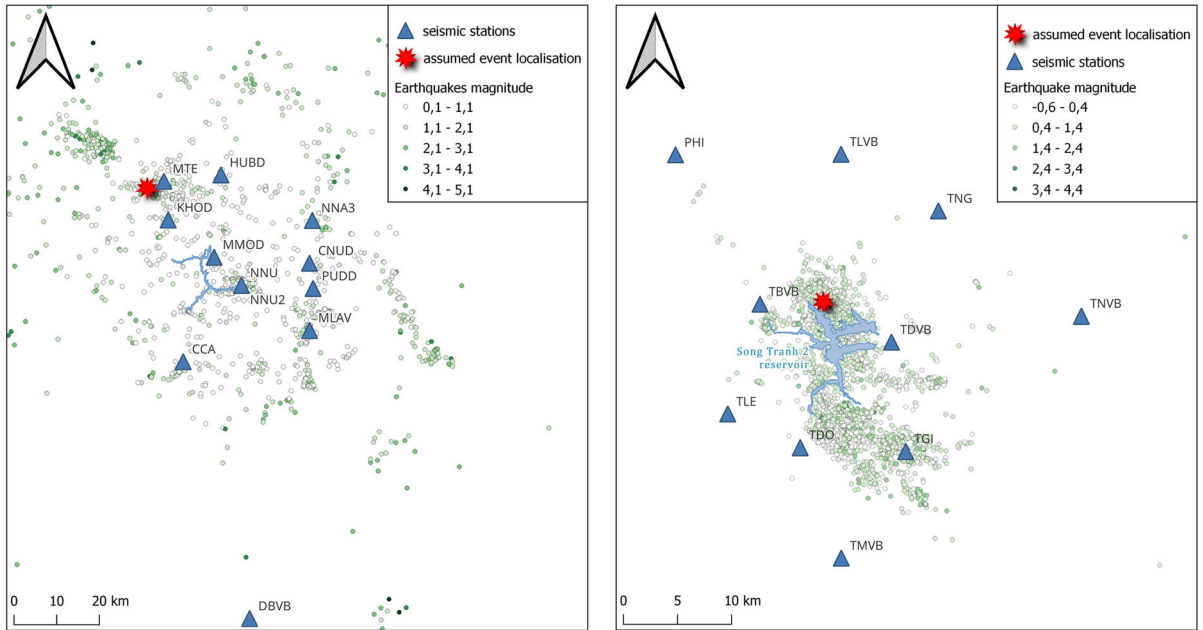


Figure 1
Map of the seismic network and seismicity of Lai Chau (left) and Song Tranh 2 area (right)

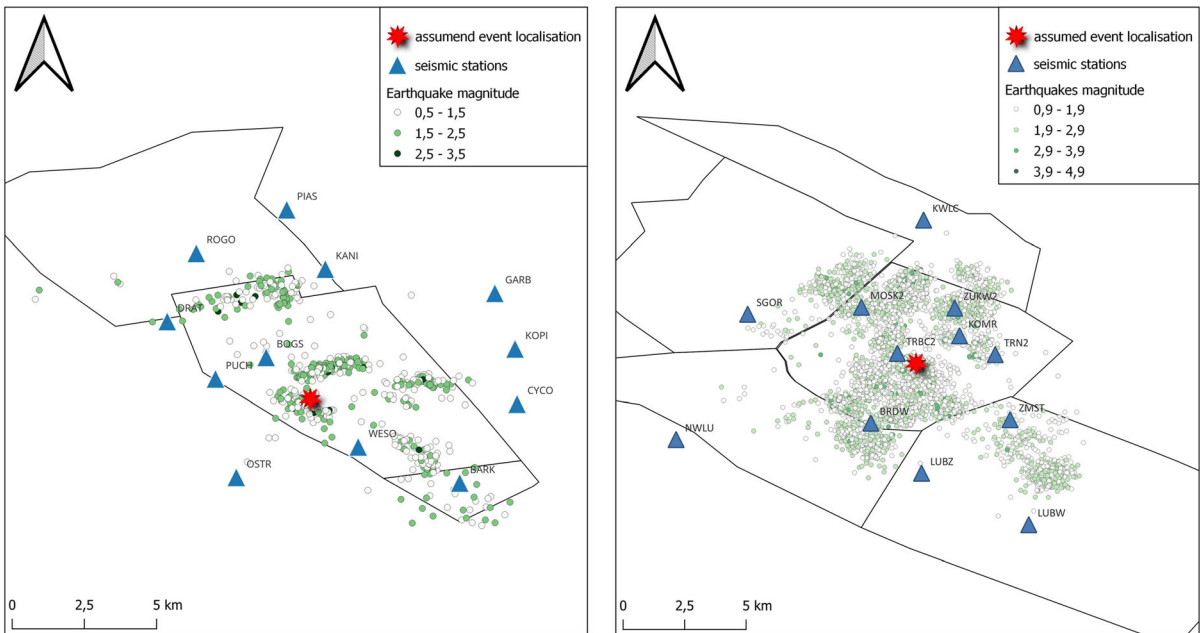


Figure 2
Map of the seismic network and seismicity of Bogdanka (left) and Rudna (right) mines area

BOgdanka mine Induced Seismicity (BOIS) is a surface network established for seismic monitoring underground coal mine Bogdanka located in the eastern Poland in Lublin Mining District. Network consist of 12 seismic stations located in the distances from 2 to 16 km from each other. Exploited coal deposits are placed at depths 500–1200 m. Mine exploit coal with the longwall mining system with caving behind the face with narrow 5 m pillars between (Philpott, 2002). Strongest event has magnitude $M = 2.9$ December 10, 2018. Average seismic activity is more than 10 events per week greater than $M = 0.5$. Geological structure is simply overlaying strata dipping to northwest with only small normal faults. The velocity model is presented on Fig. 3. Seismic data are available on Episodes Platform (IS-EPOS, 2019).

3. Methodology

Seismic moment tensor M is a nine element, symmetrical matrix with 6 independent components describing the source of earthquake. Based on the relations between displacement on the surface and

forces in the foci MT can be calculated by the inversion of N equations:

$$U^P(x, t) = \frac{\gamma \cdot \dot{M}(t - \frac{r}{\alpha}) \cdot \gamma}{4\pi\rho\alpha^3 r} l \quad (1)$$

where ρ is the average medium density, r is the source-receiver distance, α is the average velocity of the P wave, M is the seismic moment tensor, l is the P wave direction at the receiver, and γ is the P-wave direction at the source. (Aki & Richards, 2002; De Natale et al., 1987).

As the matrix has 6 independent components at least six equations (data form six stations) are required for the inversion. Full moment tensor solution can be limited to deviatoric moment tensor without volumetric changes if zero trace condition is applied. If zero determinant is additionally set the double couple solution is given. Other decomposition proposed by Jost and Herman (1989) decompose full moment tensor for isotropic (ISO), compensated linear vector dipole (CLVD) and double couple (DC) components. Such description of seismic source allows for control of quality solution and shows the complexity of mechanism. The P-wave first onset amplitude inversion is formulated in L2 norm so root-

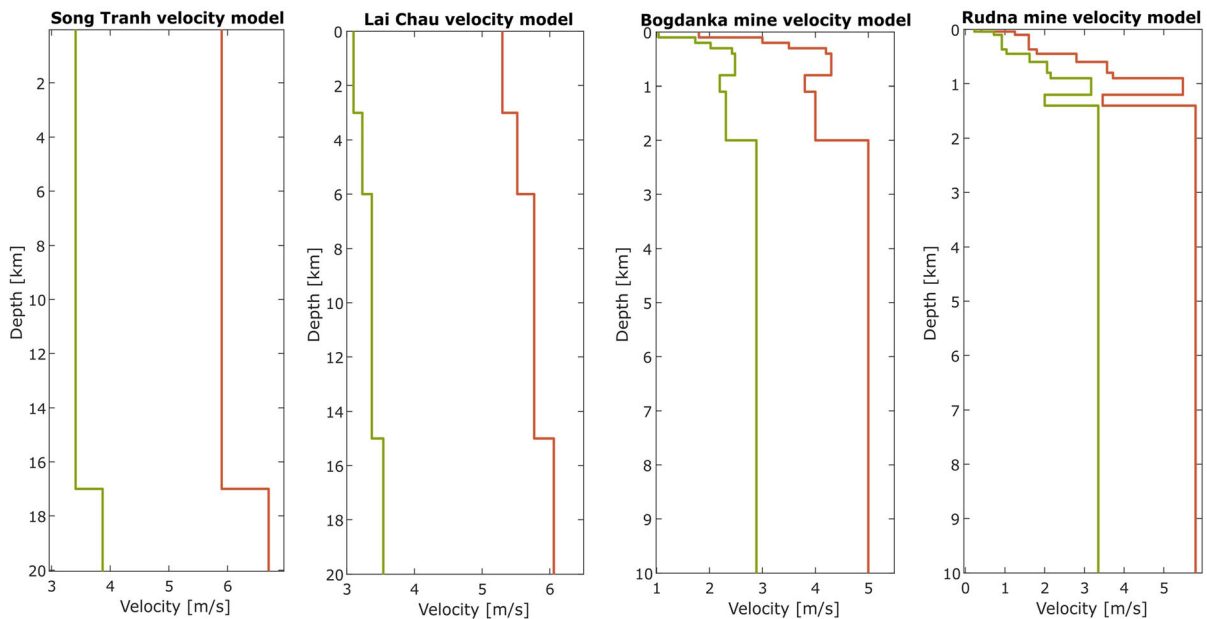


Figure 3
Velocity models of four seismic networks

mean-square (RMS) errors between measured and synthetic amplitudes are given by formula (Stierle et al., 2014a, 2014b):

$$RMS = \sqrt{\frac{\sum_{i=1}^N (U_i^{measured} - U_i^{th})^2}{\sum_i (U_i^{measured})^2}} \quad (2)$$

Model assumed for generating non shearing mechanism is tensile angle (Vavryčuk, 2001). Tensile angle is the value given in degrees describing the crack behaviour. The 0° value is slip on crack, -90° when crack is closing and $+90^\circ$ when crack opens. Tensile angle allows modelling of complex non-shearing mechanisms based on Fig. 4.

The main objective to perform synthetic tests was to check the credibility of moment tensor solutions for non-DC mechanisms by comparing assumed mechanisms with the resulting mechanism for different depths, non-DC components and various noise contamination levels. At first synthetic amplitudes

and polarity were generated. The hybridMT program allowed to generate first peak amplitudes for particular parameters of event: location, magnitude M_W , depth, fault plane strike, dip and rake, 1D velocity model and tensile angle (Kwiatek et al., 2016). Applied depths for both mine networks was: 500 m, 800 m, 1 km, 2 km, 5 km and 8 km. For artificial reservoir networks also 10 km and 15 km were calculated. The range of depths cover the shallow events recorded on the mine networks as well as the deeper events occurring in the reservoir networks, which gives the ability to compare these networks. Different tensile angles were performed, and eventually, those values for which the assumed DC component decrease every 10% were chosen. Velocity models for the area were taken from the EPISODES platform (Orlecka-Sikora et al., 2020). Further synthetic amplitudes were used to calculate moment tensors for four noise levels and the Jackknife single-station rejection tests were performed. In real application of

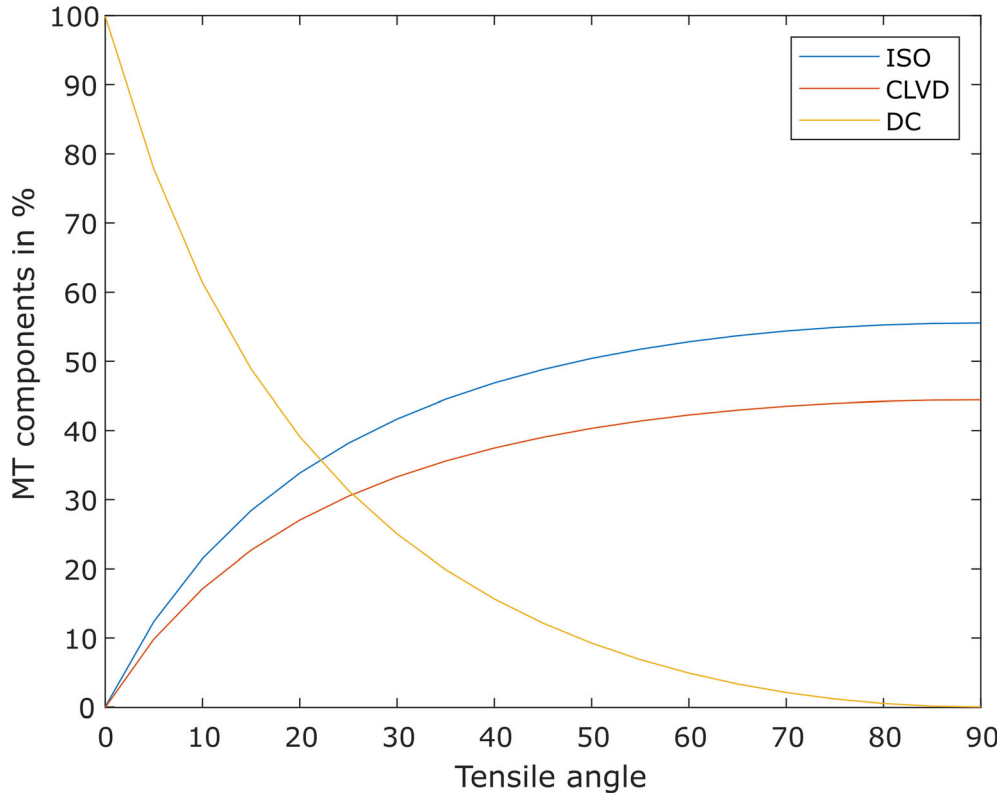


Figure 4
The MT components dependence on the tensile angle

MT inversion data from all stations are not always available. To determine if there is a crucial station in the network for stable solutions of MT for particular network the jackknife station rejection test was performed. Each time one station was rejected to check quality of MT solution for incomplete set of data. Considered levels of added synthetic Gaussian noise has average values of 10%, 20%, 30% and 40% of generated amplitudes. Each noise bootstrap were performed 100 times.

To determine if the examined MT solution is reliable three characteristics were taken into account: the Root Mean Square (RMS) values, calculated components (ISO, CLVD and DC percentage), and fault type accordance with the assumed one and stability of solutions as comparison of the nodal planes directions for full, deviatoric and DC solutions (Fig. 5).

The assumed fault geometry for Song Tranh was normal and reverse fault with $304^{\circ}/71^{\circ} \pm 108^{\circ}$ (strike/dip/rake), which is similar to most of the available solutions (see Fig. 1 Lizurek et al., 2017). The event was placed in the middle of the network, near the reservoir. Event magnitude was set to

$M_w = 3.7$. Jackknife station rejection test did not reveal crucial stations for this network.

Event fault geometry used for Lai Chau test was also normal and reverse fault with $170^{\circ}/46^{\circ} \pm 90^{\circ}$ (strike/dip/rake). The assumed magnitude was $M_w = 3.7$. Event location was set on the edge of the network, near the reservoir as no event with determined focal mechanism was located in the middle of the network as far. Jackknife station rejection test did not reveal crucial stations for this network. The strike-slip mechanisms were not considered as any other considered case allow for comparison of such solutions.

The assumed seismic source for tests in Rudna was located in the middle of the network, near TRBC station. Assumed fault plane was $170^{\circ}/46^{\circ} \pm 90^{\circ}$ (strike/dip/rake). Magnitude $M_w = 3.7$ was performed for all synthetic tests. The Jackknife single station removal test results in no influence on solutions for almost all stations. Only the TRBC station removal produce the reversed fault type in case of events below 1 km depth. TRBC is the closest station to the event location and poor focal coverage cause this station essential for correct MT inversion.

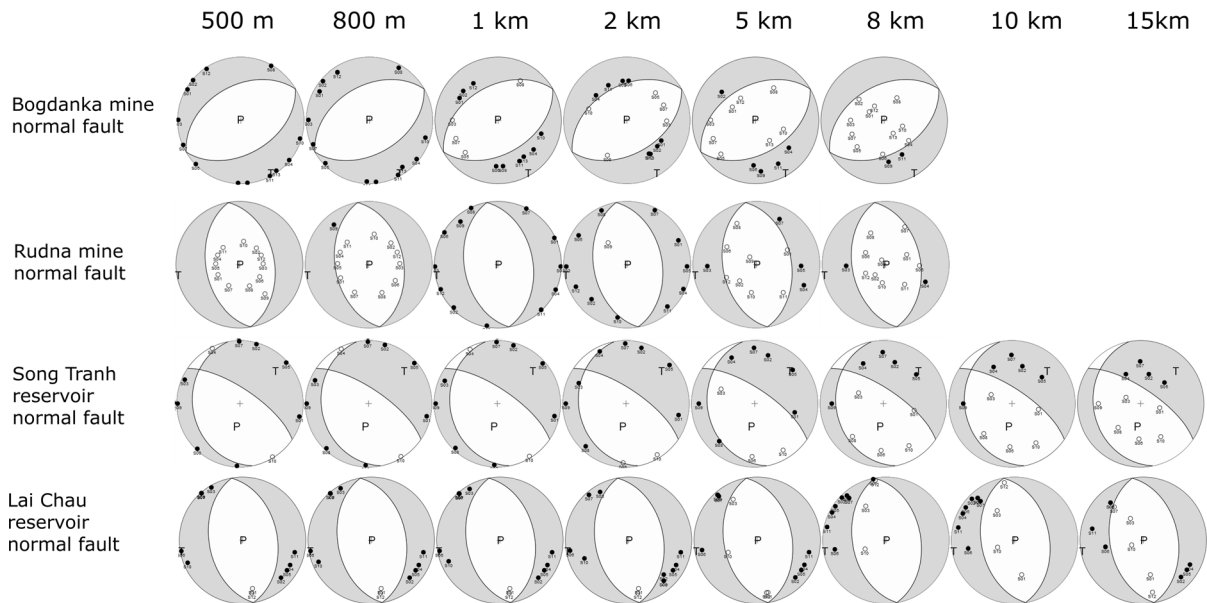


Figure 5
Focal coverage of the MT solution in depth for different networks

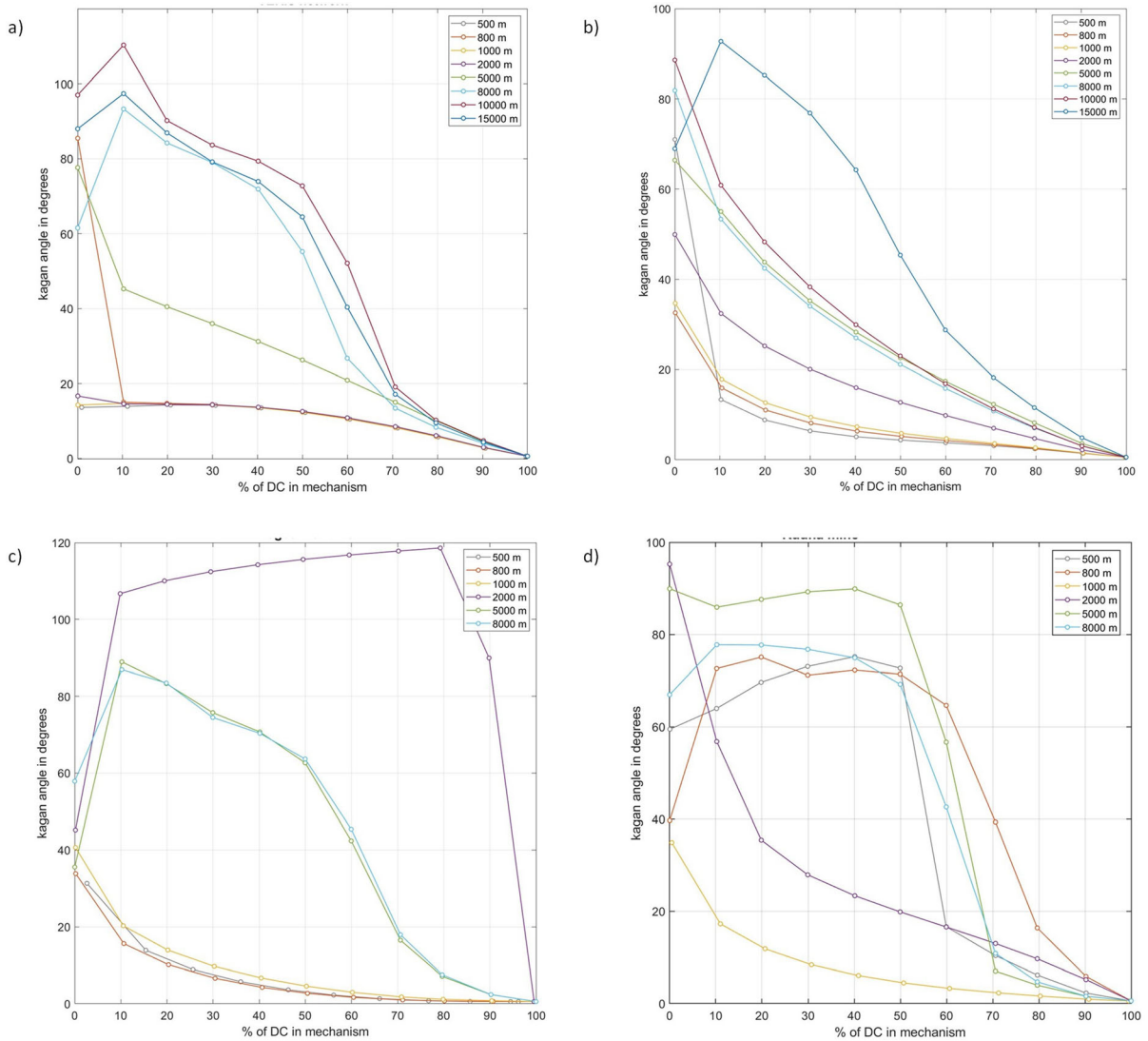


Figure 6

Rotation angle between full and deviatoric solution for assumed depths for **a** Song Tranh, **b** Lai Chau, **c** Bogdanka mine, **d** Rudna mine

For Bogdanka assumed geometry was $60^\circ/46^\circ/\pm 90^\circ$ (strike/dip/rake) as the direction the longwall faces runs. Tests were performed for two magnitudes: $M_w = 3.7$ as the comparison to other networks and $M_w = 2.9$ as the maximum registered magnitude. There were no essential differences in results for mentioned magnitudes, so further solutions for $M_w = 2.9$ are considered. Event was placed in the middle of the network in the currently active area. Jackknife station rejection test did not reveal crucial stations for this network.

4. Focal Sphere Coverage and Station Importance

For each network focal coverage depends on depth and velocity model (Fig. 5). For homogenous media in Song Tranh smooth change dependent on depth is visible. For simple models like in Lai Chau focal coverage change gradually with velocity changes. In Bogdanka focal coverage improve gradually, except 2 km switch of station locations on the sphere caused by low-velocity layer and significant change of take-off angles. Changes in focal coverage for

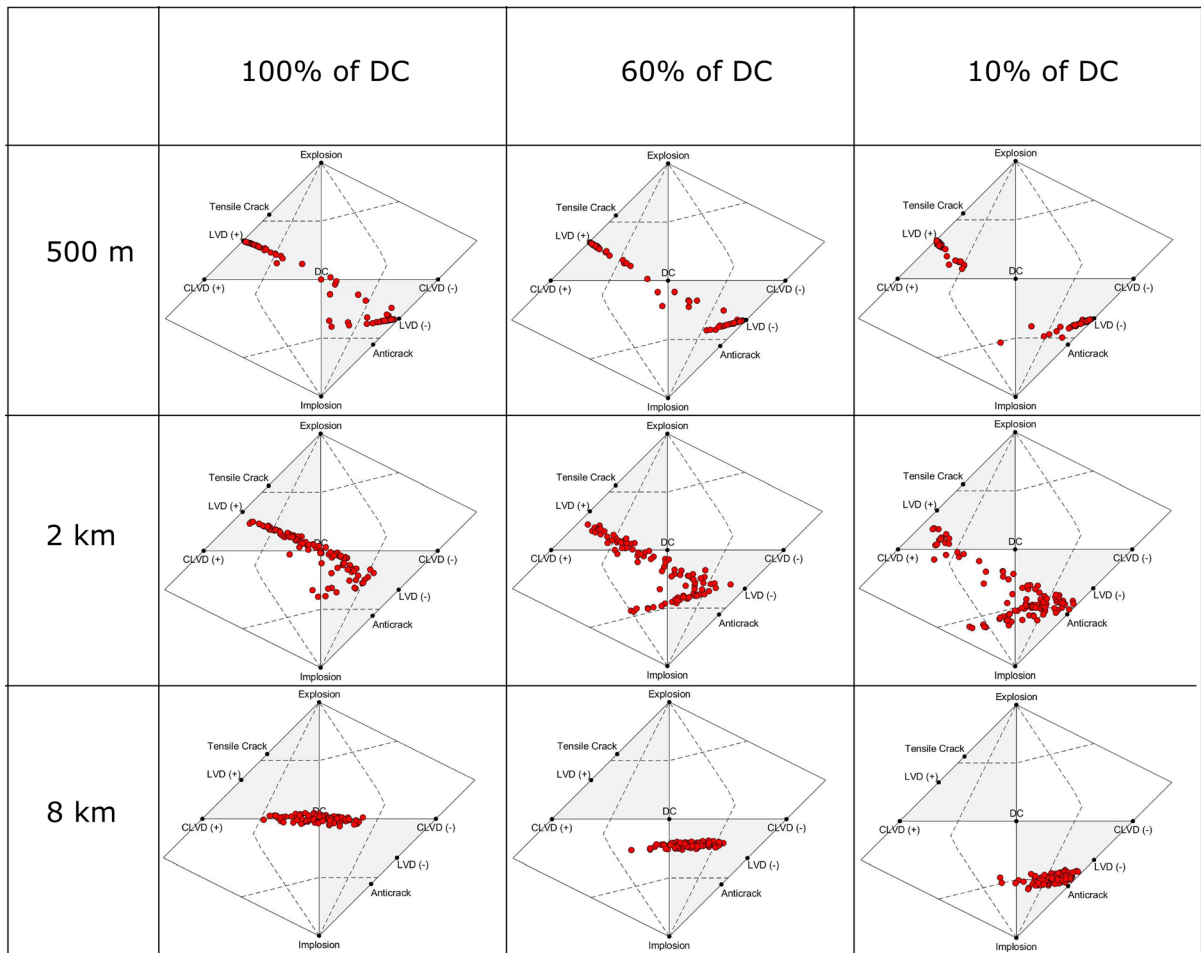


Figure 7

The Hudson plots for Song Tranh network for 500 m, 2 km and 8 km depth for three assumed DC components. Noise level 20%

events in Rudna mine reflects the complexity of the velocity model (Fig. 6).

4.1. Stability of Solutions

To determine the stability of solutions the smallest rotation angle between nodal planes for full and double couple solutions was calculated. Stability solutions were broken into categories because of their characteristics. Reservoir cases had simple velocity models with relatively high velocities. We can observe that for gradually increasing velocity like in Lai Chau deeper events are resolved slightly better than for constant velocity like in Song Tranh. The second feature is that deeper events become resolved

worse than shallow ones, especially for non-shearing events. In both cases from the depth of 5 km non shearing mechanisms are unstable. Also, the distance between event and station should be smaller than the depth of event in inhomogeneous media for optimum stations layout for MT calculations (Ren et al., 2022). Unfavourable event location on the edge of the seismic network does not influence visibly on solutions stability.

Mine stability solutions are more complicated and are linked to velocity model complexity. Shallow events in the range of 500 m–1 km in the Bogdanka area are resolved well, despite unfavourable focal coverage. In Rudna low velocities near the surface (below 3 km/s) become a substantial part of the

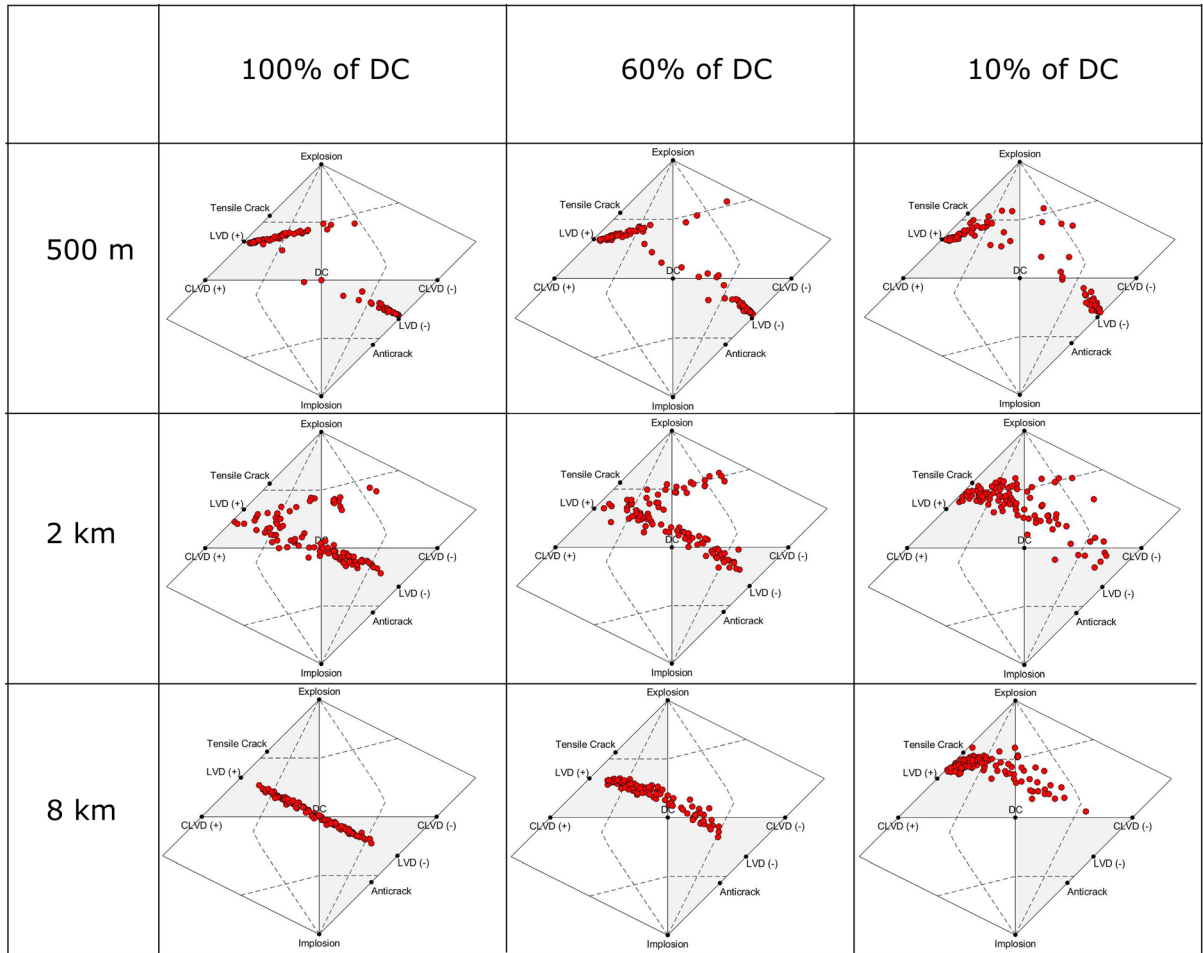


Figure 8

The Hudson plots for Lai Chau network for 500 m, 2 km and 8 km depth for three assumed DC components. Noise level 20%

velocity profile for 500 m solutions which results with unstable outcome for non-shearing events. On 2 km in Bogdanka, there is a velocity layer boundary, same is for 800 m in Rudna mine, which can explain instability for these depths. Additionally, Bogdanka's 2 km depth is the end of a thick low-velocity layer. Stable solutions on depths 1 km and 2 km in Rudna mine are visible despite unfavourable focal coverage. In both mines events deeper than 2 km exceed the event-station distance, which results with unstable outcomes for non-DC mechanisms.

4.2. Noise Bootstrap

Song Tranh noise bootstrap in case of 10% noise level for both normal and reversed fault resulted in RMS below 0.15 value. For 20% noise contamination RMS does not exceed 0.3 for normal fault geometry, but some values up to 0.4 were observed for reverse geometry. Noise level 30% resulted in RMS value up to 0.4 for both normal and reverse fault geometry. In general RMS values were increasing with the noise level and event depth increase. The similarity of MT decomposition in results to the assumed ones in tests performed for the VERIS network was the biggest for 5 km, 8 km and 10 km depths. With gaining up the noise differences in calculated components increased.

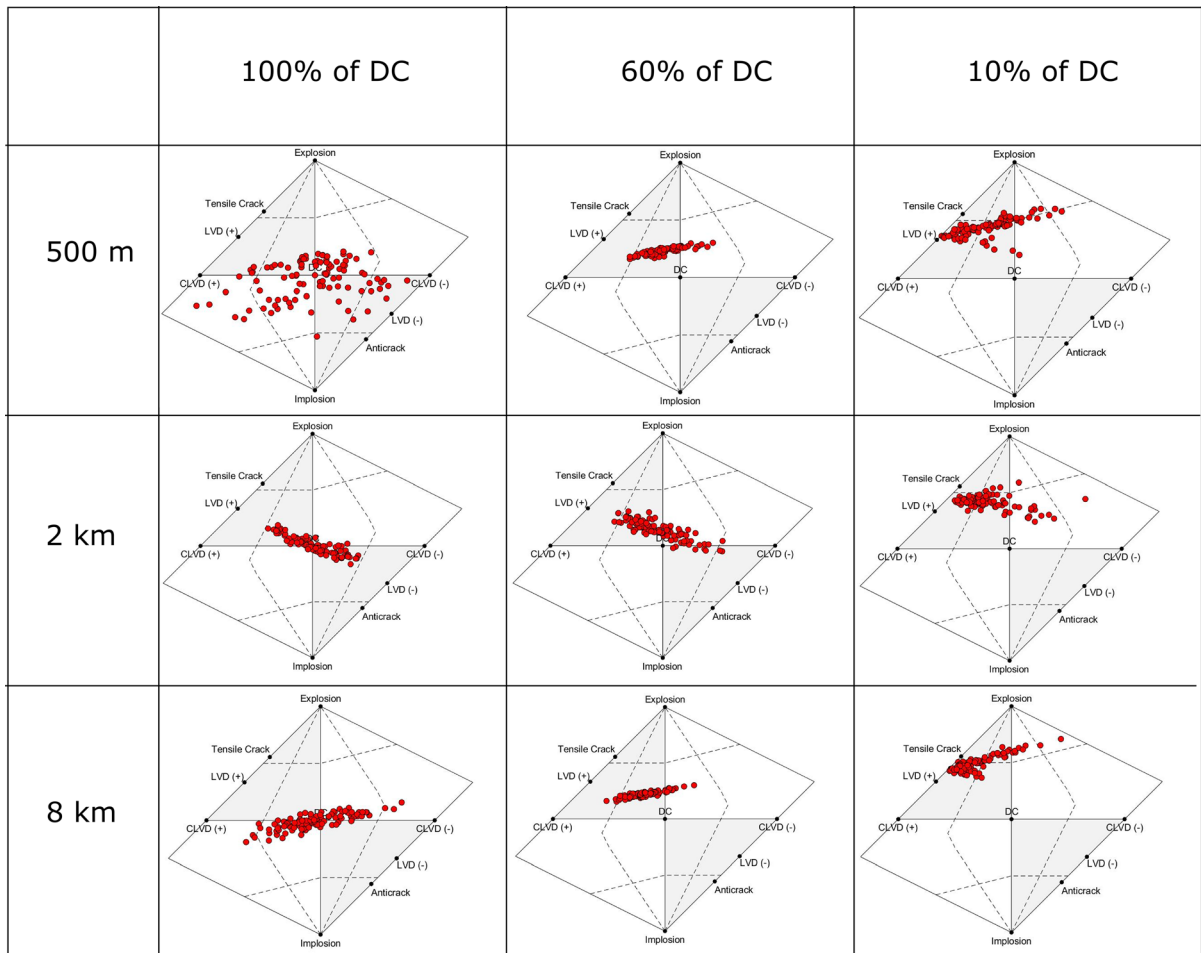


Figure 9

The Hudson plots for Rudna mine network for 500 m, 2 km and 8 km depth for three assumed DC components. Noise level 20%

For event depths more than 2 km the differences were small and for shallower events become more scattered through a whole range of MT solutions. Dissipation of solutions increased also with non-DC components participation, up to occurring two clusters of solutions for 10% of DC: the first one for correct solutions and the second one for the opposite solutions (Fig. 7). There was no visible distinction in MT decomposition results and stability between normal and reverse fault geometry.

Lai Chau tests RMS error value was the same for the normal and thrust fault for particular noise levels, from 0.15 RMS error for 10% noise level, for 20% noise RMS error was below 0.3, for 30% and 40% noise contamination RMS was mostly below 0.5. The

RMS error increased with depth increasing and was worse for mechanisms with about 50% of non-DC components compared to other mechanisms with the same depth and noise level. Gradual improvement of the components results was visible with depth increase, with rapid improvement at 5 km depth (Fig. 8). For 500 m two clusters of solutions are observed, and the most scattered are 2 km results. For 10% noise level results tends to align in case of shallow events, but dispersion of results for higher noise contamination cause disappearance of this feature.

Rudna noise bootstrap in case of 10% noise level for both fault geometries resulted in RMS below 0.15 value. For 20% noise contamination RMS does not

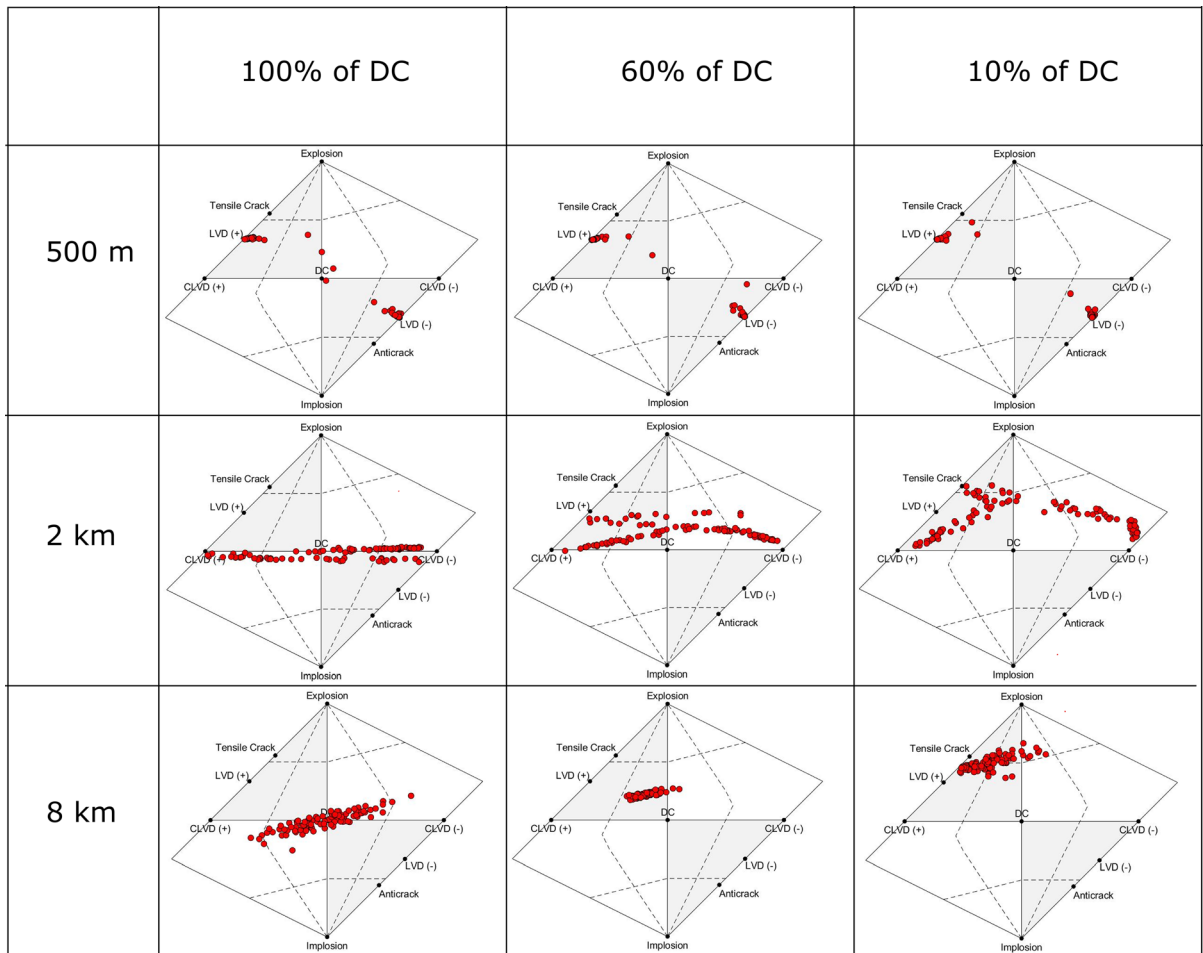


Figure 10

The Hudson plots for Bogdanka mine network for 500 m, 2 km and 8 km depth for three assumed DC components. Noise level 20%

exceed 0.3. Noise level 30% resulted in an RMS value up to 0.4 for normal fault geometry and 0.5 for reverse fault geometry. 40% noise level results in up to 0.6 RMS however, there were single cases that exceeded 0.4. In general RMS values were increasing with noise level increment. MT components in tests performed for the mine network were resolved well for almost all depth ranges. Very shallow events on 500 m depth were scattered the most and solutions for the DC mechanisms were resolved with many nonphysical solutions (Fig. 9). With increasing depth MT components were resolved with better consistency with the assumed ones, except for the 1 km depth where many nonphysical solutions were noticed.

Bogdanka both normal and reverse fault noise bootstrap for 10% of noise contamination was resolved with RMS errors below 0.2, for 20% noise RMS was below 0.3, for 30% noise below 0.4 and for 40% noise level RMS error was mostly below 0.5 with few cases of 0.6. The value of RMS error increases with noise contamination increment. In case of events placed on velocity layer boundaries the improvement in RMS values for pure shear mechanism were observed. The influence of velocity model is visible in obtained solutions. Solutions on depth 500 m was resolved with two clusters no matter what kind of mechanism was assumed (Fig. 10). Visible is also dissipation in calculated components for 2 km depth with many nonphysical solutions. Similar

consistency of MT components with comparison to assumed ones as for 2 km was noticed for 1 km solutions. Best solutions were obtained for 5 km depth, as 8 km become more scattered again. With increasing noise level solutions scattered more, however mechanisms about 50% of DC seems less sensitive for noise contamination.

5. Conclusions

In this work abilities of four networks with different velocity models to provide good quality MT inversion were compared. Synthetic tests revealed low velocity layer impact on solutions stability. There was observed worse stability of solutions for mine networks because of complexity of velocity model. Also, instability in solutions if located on the velocity layer boundary was observed. Instability in solutions were observed especially if depth of event was greater than biggest event-station distance, which is in accordance with another research (Ren et al., 2022). Too shallow events on 500 m depth for all networks except Rudna mine were resolved with incorrect components with tendency to form two clusters of solutions if noise contamination was applied. Even if RMS error value is small solution can be wrong. A noise level above 20% of the registered amplitude cause significant deterioration in solutions quality.

The two networks established for artificial reservoir monitoring, Lai Chau and Song Tranh, allow for stable and reliable MT inversion within the range of depths events are located. Limitations of MT inversion for these networks seems to be mainly connected with a shallow and non-DC type of events, which are unlikely to occur in reservoir triggered seismicity on existing tectonic discontinuities. Location of the event on the network edge influence rather on the components results, but not on the stability of the solution.

Rudna network performed well in resolving components at depth for 800 m which corresponds with exploitation level. However, the solutions of events with non-DC components are unstable for all depths except 1 km, where is a visible influence of low-velocity layer in components results. There is no

depth with both correct stability and components results for non-shearing mechanisms. Because of this feature and non-DC characteristic of mine tremors MT inversion result should be considered carefully, and should not be considered without additional information.

Bogdanka mine network should not be used for routine MT inversion without additional information. Tests performed on the Bogdanka network results in the right component solutions only for events deeper than 2 km, which are unlikely to occur in the mining area and results of stability for non-DC events also cause these solutions unreliable. A thick low-velocity layer makes solutions unstable or nonphysical. In comparison with test results obtained for Rudna mine the influence of the detailed velocity model near the surface should be examined to determine if inclusion of this model can improve MT solution quality.

As the MT inversion is a common tool in seismology, the P-wave amplitude inversion method limits the use of data with low noise-to-signal ratio, and events on depths not exceeding the maximum event-station distance. Knowledge about applied velocity models can be crucial as the influence of high velocity gradient can cause wrong components determination with seemingly correct solution.

Acknowledgements

This work was partially financed from Polish National Science Centre Grant no. 2021/41/B/ST10/02618. Team was supported by a subsidy from the Polish Ministry of Science and Higher Education for the Institute of Geophysics, Polish Academy of Sciences.

Author Contributions The study conception was made by GL. Methodology, tests design and analysis was made by AT. The first draft of the manuscript was written by AT and all authors commented on previous versions of the manuscript. The supervision was made by GL. All authors read and approved the final manuscript.

Funding

This article was funded by Polish National Science Centre Grant no.2021/41/B/ST10/02618. Team was supported by a subsidy from the Polish Ministry of Science and Higher Education for the Institute of Geophysics, Polish Academy of Sciences.

Data and Resources

The seismological data is available from the repository of EPOS Thematic Core Service Anthropogenic Hazards (EPISODES platform) at: <https://episodesplatform.eu/?lang=pl#episode:BOGDANKA>, <https://episodesplatform.eu/?lang=en#episode:LGCD>, https://episodesplatform.eu/?lang=pl#episode:SONG_TRANH, https://episodesplatform.eu/?lang=pl#episode:LAI_CHAU (last accessed in March 2023).

Declarations

Conflict of interest The authors declare no competing interests.

Open Access This article is licensed under a Creative Commons Attribution 4.0 International License, which permits use, sharing, adaptation, distribution and reproduction in any medium or format, as long as you give appropriate credit to the original author(s) and the source, provide a link to the Creative Commons licence, and indicate if changes were made. The images or other third party material in this article are included in the article's Creative Commons licence, unless indicated otherwise in a credit line to the material. If material is not included in the article's Creative Commons licence and your intended use is not permitted by statutory regulation or exceeds the permitted use, you will need to obtain permission directly from the copyright holder. To view a copy of this licence, visit <http://creativecommons.org/licenses/by/4.0/>.

Publisher's Note Springer Nature remains neutral with regard to jurisdictional claims in published maps and institutional affiliations.

REFERENCES

- Aki K., Richards P. (2002). *Quantitative seismology*, 2nd Ed. University Science Books
- Bentz, S., Martínez Garzon, P., Kwiatek, G., Bohnhoff, M., & Renner, J. (2018). Sensitivity of full moment tensors to data preprocessing and inversion parameters: A case study from the Salton Sea Geothermal field. *Bulletin of the Seismological Society of America*, 108(2), 588–603.
- Cesca, S., Buforn, E., & Dahm, T. (2006). Amplitude spectra moment tensor inversion of shallow earthquakes in Spain. *Geophysics Journal International*, 166(2), 839–854. <https://doi.org/10.1111/j.1365-246X.2006.03073.x>
- Cesca, S., Rohr, A., & Dahm, T. (2013). Discrimination of induced seismicity by full moment tensor inversion and decomposition. *Journal of Seismology*, 17, 147–163. <https://doi.org/10.1007/s10950-012-9305-8>
- D'Amico, S. (2018). Preface. In S. D'Amico (Ed.), *Moment tensor solutions: A useful tool for seismotectonics*. Springer natural hazards (p. 5). Springer.
- Dahm, T., Becker, D., Bischoff, M., Cesca, S., Dost, B., Fritschen, R., Hainzl, S., Klose, C. D., Kuhn, D., Lasocki, S., Meier, Th., Ohrnberger, M., Rivalta, E., Wegler, U., & Husen, S. (2013). Recommendation for the discrimination of human-related and natural seismicity. *Journal of Seismology*, 17(1), 197–202.
- De Natale, G., Iannaccone, G., Martini, M., et al. (1987). Seismic sources and attenuation properties at the Campi Flegrei volcanic area. *PAGEOPH*, 125, 883–917. <https://doi.org/10.1007/BF00879360>
- Ekström, G., Nettles, M., & Dziewoński, A. M. (2012). The global CMT project 2004–2010: Centroid-moment tensors for 13,017 earthquakes. *Physics of the Earth and Planetary Interiors*, 200–201, 1–9. <https://doi.org/10.1016/j.pepi.2012.04.002>
- IS EPOS. (2017). Epizod: LGCD, <https://episodesplatform.eu/#episode:LGCD>, https://doi.org/10.25171/InstGeoph_PAS_ISEPOS-2017-006
- IS EPOS. (2017). Epizod: SONG TRANH, https://episodesplatform.eu/#episode:SONG_TRANH, https://doi.org/10.25171/InstGeoph_PAS_ISEPOS-2017-002
- IS EPOS. (2018). Epizod: LAI CHAU, https://episodesplatform.eu/#episode:LAI_CHAU, https://doi.org/10.25171/InstGeoph_PAS_ISEPOS-2018-012
- Fletcher, B. J., & McGarr, A. (2005). Moment tensor inversion of ground motion from mining-induced earthquakes, Trail Mountain, Utah. *Bulletin of the Seismological Society of America*, 95(1), 48–57.
- Fojtíková, L., Vavryčuk, V., Cipciar, A., & Madarás, J. (2010). Focal mechanisms of micro-earthquakes in the Dobrá Voda seismoactive area in the Malé Karpaty Mts. (Little Carpathians), Slovakia. *Tectonophysics*, 492, 213–229. <https://doi.org/10.1016/j.tecto.2010.06.007>
- Ford, S. R., Dreger, D. S., & Walter, W. R. (2009). Identifying isotropic events using a regional moment tensor inversion. *Journal of Geophysical Research*, 114, B01306. <https://doi.org/10.1029/2008JB005743>
- Ford, S. R., Dreger, D. S., & Walter, W. R. (2010). Network sensitivity solutions for regional moment-tensor inversions. *Bulletin of the Seismological Society of America*, 100(5A), 1962–1970. <https://doi.org/10.1785/0120090140>
- Gahalaut, K., Tuan, A. T., & Purnachandra, R. N. (2016). Rapid and delayed earthquake triggering by the song Tranh 2 Reservoir, Vietnam. *Bulletin of the Seismological Society of America*, 106(5), 2389–2394. <https://doi.org/10.1785/0120160106>
- Gibowicz, S. J., & Kijko, A. (1994). *An introduction to mining seismology*. Academic Press Inc.
- Hardebeck, J. L., & Michael, A. J. (2006). Damped regional-scale stress inversions: Methodology and examples for southern

- California and the Coalinga aftershock sequence. *Journal of Geophysical Research*, *111*, B11310. <https://doi.org/10.1029/2005JB004144>
- Heimann, S., Gonzalez, A., Wang, R., Cesca, S., & Dahm, T. (2013). Seismic characterization of the Chelyabinsk Meteor's terminal explosion. *Seismological Research Letters*, *84*(6), 1021–1025. <https://doi.org/10.1785/0220130042>
- IS-EPOS. (2019). Epizod: BOGDANKA. <https://episodesplatform.eu/#episode:BOGDANKA>, https://doi.org/10.25171/InstGeoph_PAS_ISEPOS-2019-001
- Jost, M. L., & Herrmann, R. B. (1989). A Student's Guide to and Review of Moment Tensors. *Seismological Research Letters*, *60*(2), 37–57. <https://doi.org/10.1785/GSSRL.60.2.37>
- Kwiatk, G., Martínez-Garzón, P., & Bohnhoff, M. (2016). HybridMT: A MATLAB/shell environment package for seismic moment tensor inversion and refinement. *Seismological Research Letters*. <https://doi.org/10.1785/0220150251>
- Lasocki, S., & Orlecka-Sikora, B. (2008). Seismic hazard assessment under complex source size distribution of mining-induced seismicity. *Tectonophysics*, *456*, 28–37. <https://doi.org/10.1016/j.tecto.2006.08.013>
- Lizurek, G., Leptokaropoulos, K., Wiszniowski, J., Van Giang, N., Nowaczyńska, I., Plesiewicz, B., Van Quoc, D., & Tyimińska, A. (2021). Seasonal trends and relation to water level of reservoir-triggered seismicity in Song Tranh 2 reservoir, Vietnam. *Tectonophysics*. <https://doi.org/10.1016/j.tecto.2021.229121>
- Lizurek, G., Wiszniowski, J., Van Giang, N., Plesiewicz, B., & Van, D. Q. (2017). Clustering and Stress Inversion in the Song Tranh 2 Reservoir, Vietnam. *Bulletin of the Seismological Society of America*, *107*(6), 2636–2648.
- Lizurek, G., Wiszniowski, J., Giang, N., Van, D., Dung, L., Tung, V., & Plesiewicz, B. (2019). Background seismicity and seismic monitoring in the Lai Chau reservoir area. *Journal of Seismology*. <https://doi.org/10.1007/s10950-019-09875-6>
- Martinez Garzon, P., Kwiatek, G., Ickrath, M., & Bohnhoff, M. (2014). MSATSI: A MATLAB package for stress inversion combining solid classic methodology, a new simplified user-handling, and a visualization tool. *Seismological Research Letters*, *85*(4), 896–904.
- Miller, A. D., Foulger, G. R., & Julian, B. R. (1998). Non-double-couple earthquakes, 2 observations. *Reviews of Geophysics*, *36*, 551–568.
- Orlecka-Sikora, B., Lasocki, S., Kocot, J., et al. (2020). An open data infrastructure for the study of anthropogenic hazards linked to georesource exploitation. *Scientific Data*, *7*, 89. <https://doi.org/10.1038/s41597-020-0429-3>
- Philpott, K. D. (2002). Evaluation of the Bogdanka Mine, Poland. *Polish Geological Institute Special Papers*, *7*, 199–206.
- Ren, Y., Vavryčuk, V., Gao, Y., Wu, S., & Gan, Y. (2022). Efficiency of surface monitoring layouts for retrieving accurate moment tensors in hydraulic fracturing experiments. *Pure and Applied Geophysics*. <https://doi.org/10.1007/s00024-022-03122-9>
- Romanowicz, B., Dreger, D., Pasyanos, M., & Uhrhammer, R. (1993). Monitoring of strain release in central and northern California using broadband data. *Geophysical Research Letters*, *20*, 1643–1646.
- Rudajev, V., & Šílený, J. (1985). Seismic events with non-shear component II. Rock bursts with implosive source component. *PAGEOPH*, *123*, 17–25.
- Šílený, J., Jechumtalova, Z., & Dorbath, C. (2014). Small Scale earthquake mechanisms induced by fluid injection at the enhanced geothermal system reservoir Soultz (Alsace) in 2003 using alternative source models. *Pure Applied Geophysics*, *171*(10), 2783–2804. <https://doi.org/10.1007/s00024-013-0750-2>
- Stierle, E., Bohnhoff, M., & Vavryčuk, V. (2014b). Resolution of non-double-couple components in the seismic moment tensor using regional networks—II: Application to aftershocks of the 1999 Mw 7.4 Izmit earthquake. *Geophysics Journal International*. <https://doi.org/10.1093/gji/ggt503>
- Stierle, E., Vavryčuk, V., Šílený, J., & Bohnhoff, M. (2014a). Resolution of non-double-couple components in the seismic moment tensor using regional networks—I: A synthetic case study. *Geophysical Journal International*. <https://doi.org/10.1093/gji/ggt502>
- Vavryčuk, V. (2001). Inversion for parameters of tensile earthquakes. *Journal of Geophysics Research*, *106*(B8), 16339–16355. <https://doi.org/10.1029/2001JB000372>
- Vavryčuk, V. (2018). Moment tensor in anisotropic media: a review. In S. D'Amico (Ed.), *Moment tensor solutions: a useful tool for seismotectonics*. Springer natural hazards (pp. 29–55). Springer.
- Vavryčuk, V., & Kim, G. S. (2014). Nonisotropic radiation of the 2013 North Korean nuclear explosion. *Geophysical Research Letters*, *41*, 7048–7056. <https://doi.org/10.1002/2014GL061265>
- Wiejacz, P. (1992). Calculation of seismic moment tensor for mine tremors from the Legnica- Głogów Copper Basin. *Acta Geophysica Polonica XI*, *2*, 103–122.
- Wiszniowski, J., Giang, N. V., Plesiewicz, B., Lizurek, G., Van, D. Q., Khoi, L. Q., & Lasocki, S. (2015). Preliminary results of anthropogenic seismicity monitoring in the region of Song Tranh 2 Reservoir, Central Vietnam. *Acta Geophysica*, *63*(3), 843–862.
- Zahradnik, J., & Sokos, E. (2018). ISOLA code for multiple-point source modeling—Review. In S. D'Amico (Ed.), *Moment tensor solutions: A useful tool for seismotectonics*. Springer natural hazards (pp. 1–28). Springer.